The effect of microstructure on toughness of Ni/Al$_2$O$_3$ composites prepared by spark plasma sintering

Qinfang Yan [a,b], Zhengren Huang [a,*], Guillaume Yangshu Wang [c], Dongliang Jiang [a]

[a] *Shanghai Institute of Ceramics, Chinese Academy of Sciences, 1295 Road Dingxi, Shanghai 200050, China*
[b] *Graduate School of the Chinese Academy of Sciences, Beijing 100049, China*
[c] *Centre d'Etudes de Chimie Métallurgique, C.N.R.S., Vitry sur Seine 94407, France*

Abstract

Dense Ni/Al$_2$O$_3$ composites with different microstructures were fabricated using the spark plasma sintering technique. The toughness of the composites is improved by 49% when a larger percentage of nickel particles are present within the alumina grains. Microcracks and dislocations caused by nickel were observed by transmission electron microscopy and crack deflection and ductile particle bridging by scanning electron microscopy. The thermal stress and critical grain size of the second phase were calculated, to explain the initiation of microcracks and the toughening mechanisms are discussed.
© 2007 Elsevier B.V. All rights reserved.

Keywords: Alumina; Nickel; Microstructure; Toughness

1. Introduction

Ceramics are widely used in industry but the principal limitation is their brittleness, especially when the material is used in structural applications. It is well known that the toughness can be improved significantly by dispersing a second phase into the ceramic matrix or grain boundaries. The most significant achievements with this approach have been reported by Niihara and Nakahira [1,2] who first revealed a dispersion of 5 vol.% of silicon carbide in an alumina matrix which increased its strength greatly but toughness only modestly. The toughening mechanisms of the second phase, such as crack deflection toughening [3,4], crack bridged toughening [5–8], microcrack toughening [1,2] and residual stress toughening [9,10] have all been investigated.

Besides the study on silicon carbide inclusion, many investigations have been carried out on metal/ceramic nanocomposites such as Ni/Al$_2$O$_3$ [11,12], W/Al$_2$O$_3$ [13], Fe/Al$_2$O$_3$ [14] and Mo/Al$_2$O$_3$ [15]. Nickel has attracted particular attention because

it generally results in improved mechanical properties and also novel electric and magnetic properties. Most work considers the toughening mechanisms of nickel particles in Ni/Al$_2$O$_3$ composites and many explanations are presented. Tuan and Brook [16] observed the bridging and debonding nickel particles in Ni/Al$_2$O$_3$ composites, which fulfilled the two conditions in order for the plastic deformation [17]. Similarly, Sekino et al. [12] observed crack deflection and accompanying crack-fractured surface interactions, such as interlock bridging. However, it was considered that the plasticity of nickel metal had a minor role in the toughening mechanisms due to the weak interface, which was not capable of transferring external stresses to the nickel dispersions. Kolhe et al. [10,18] analyzed the effect of residual thermal stresses on the interfacial bonding in Ni/Al$_2$O$_3$ composites and calculated the critical size of spherical nickel particle for interfacial crack extension using experimental and theoretical thermal stresses, respectively. He also compared the critical size with the size calculated using Ito's model [19]. It was calculated that the critical particle radius for crack initiation is from 1.3 to 9.5 μm, compared with an experimental value of 0.75 μm.

In the present work, dense Ni/Al$_2$O$_3$ composites with different microstructures were prepared by spark plasma sintering (SPS). The microstructure and mechanical properties, especially toughness, were studied and the toughening mechanisms are

* Corresponding author at: Shanghai Institute of Ceramics, Chinese Academy of Sciences, 1295 Road Dingxi, Shanghai 200050, China.
Tel.: +86 21 52414323; fax: +86 21 52413903.
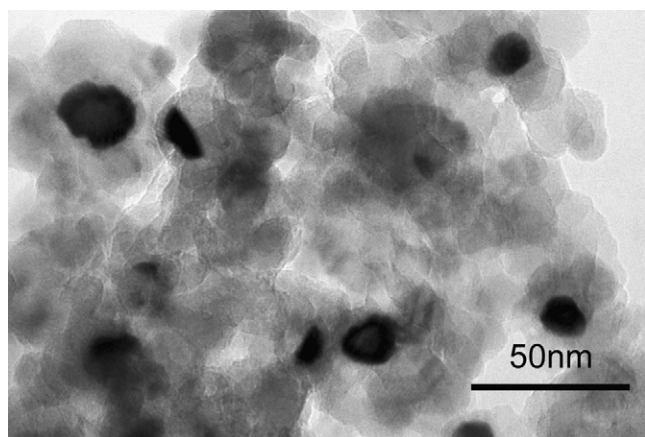 *E-mail address:* zhrhuang@mail.sic.ac.cn (Z. Huang).

Fig. 1. TEM image of the Ni/Al$_2$O$_3$ powders reduced in H$_2$ atmosphere at 700 °C for 2 h.

Fig. 2. XRD patterns of the starting γ-Al$_2$O$_3$ powders, the Ni/Al$_2$O$_3$ powders reduced in hydrogen atmosphere at 700 °C and the Ni/Al$_2$O$_3$ composites sintered by SPS at 1250 °C for 3 min, respectively.

discussed. A particle with the size of about 300 nm initiating microcrack and several dislocations beside nickel particles were observed together with crack deflection and crack bridged ductile particle. The residual stress in the composites and the critical particle size were calculated using sealing's model [20].

2. Experimental procedure

Ni/Al$_2$O$_3$ powders were prepared using γ-Al$_2$O$_3$ powders with an average particle size of 20 nm (Shanghai Wusong Fertilizer Co., China), Ni(NO$_3$)$_2$·6H$_2$O (99.9%) and NH$_4$HCO$_3$ (99.9%) as starting materials. In Li's report [21], Ni/Al$_2$O$_3$ composites with 5 vol.% Ni content had an excellent combination of mechanical properties. Thus a 5 vol.% Ni content was adopted in the present work. Ni(NO$_3$)$_2$·6H$_2$O, γ-Al$_2$O$_3$ and PEG 6000 dispersant (1 wt.%) were firstly mixed in distilled water and ball milled for 48 h with alumina balls. NH$_4$HCO$_3$ solution was then added to the as-prepared slurry during vigorous stirring. The slurry was filtered and thoroughly washed with distilled water and ethanol. The precipitants were dried in air for 48 h, calcined in air at 450 °C for 1 h and reduced in a H$_2$ atmosphere at 700 °C for 2 h. Fig. 1 shows the transmission electron microscopy (TEM) image of as-prepared powders, with nickel particles distributed homogeneously in the alumina matrix. The sizes of spherical nickel (black) and alumina particles are both around 20 nm.

The as-prepared powders were placed in a graphite mold and a 50 MPa pressure was applied. The compact block was sintered in SPS facilities (SPS 2040, Sumitomo Coal Mining Co. Ltd., Japan) at 1250 °C for 3 min with heating rates of about 200 °C/min (Ni05-1) and 100 °C/min (Ni05-2). Pure γ-Al$_2$O$_3$ powders were also sintered in similar conditions by SPS at 1310 °C for 3 min (Ni00).

The phase characterization was performed by X-ray diffraction (XRD) using Cu Kα (λ = 0.15406 nm) radiation. The microstructure was observed by scanning electron microscopy (SEM, LEO Gemini 1530, Germany) and TEM (FEI Tecnai F20, Holland). The density was obtained by using Archimedes method. Sintered samples were cut into rectangular bar specimens (2 mm × 2.5 mm × 20 mm) and the bending strength was determined by the three-point bending test (Wison-Wolpert Tukon 2100B, MA). The fracture toughness was measured by the indentation fracture technique using a micro-Vickers diamond indenter (Akashi Avk-A, Japan) with a 10 kg load. The values of density, bending strength and fracture toughness were averaged from at least five specimens.

3. Results and discussion

3.1. Phase characterization of the starting powders, as-prepared Ni/Al$_2$O$_3$ powders and composites

Fig. 2 shows the XRD patterns of the starting γ-Al$_2$O$_3$ powders, the powders reduced at 700 °C in hydrogen atmosphere
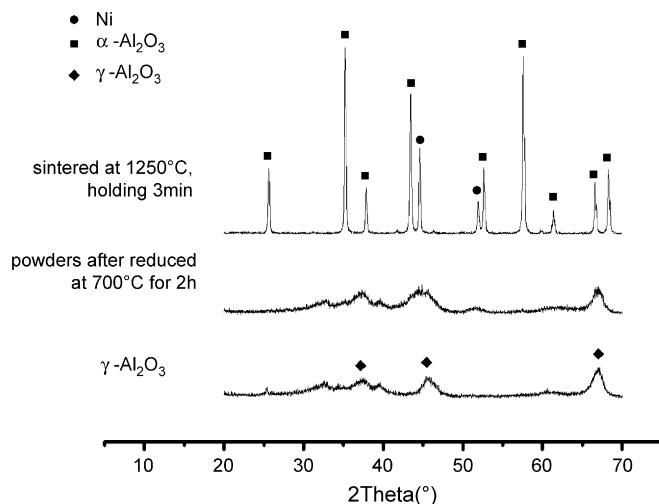
and the composites sintered by SPS at 1250 °C for 3 min. It shows that after reduction, alumina retains in the γ-Al$_2$O$_3$ phase and the nickel phase appears. However, γ-Al$_2$O$_3$ is completely transformed into α-Al$_2$O$_3$ after the SPS process.

3.2. Mechanical properties of the Ni/Al$_2$O$_3$ composites

Table 1 shows the mechanical properties of Ni00, Ni05-1 and Ni05-2. It shows that the sintering temperature decreases from 1310 to 1250 °C and the fracture toughness increases with the addition of nickel particles, at the same time, the bending strength decreases slightly while the relative densities are almost the same. The toughness of Ni05-1 has been improved by 49% compared to that of pure alumina, which is higher than that of Ni05-2 (22%). The toughening mechanisms will be discussed in detail through the study of the microstructure later.

3.3. Microstructure of the composites

Fig. 3 shows TEM images of Ni05-1 and Ni05-2 sintered at 1250 °C for 3 min by SPS. Fig. 3(a) shows that a few nickel particles (black) are in alumina grains but the vast majority is at grain boundaries in Fig. 3(b). We note that the alumina grain sizes in Ni05-1 are a little larger than those in Ni05-2. This must be due to the different sintering rate. With rapid sintering, the higher forcing energy makes more nickel particles enter the

Table 1
The densities and the mechanical properties of alumina and Ni/Al$_2$O$_3$ composites with 5 vol.% nickel content

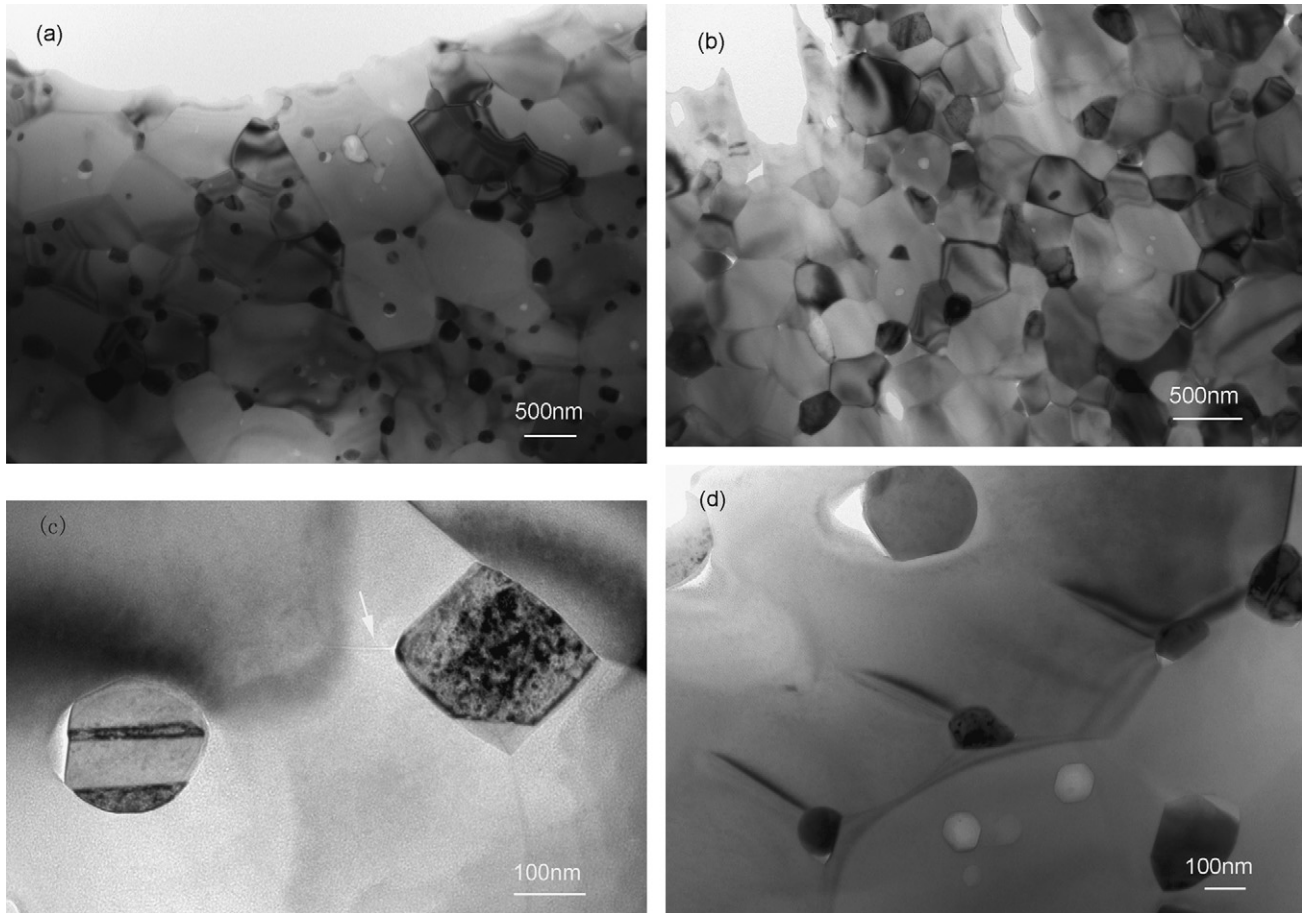|	Relative density (%)	Fracture toughness (MPa m$^{1/2}$)	Bending strength (MPa)
Ni00	96.2 ± 1.4	3.51 ± 0.41	602.55 ± 75.32
Ni05-1	96.4 ± 0.4	5.24 ± 0.17	585.58 ± 56.06
Ni05-2	96.2 ± 0.4	4.29 ± 0.29	446.81 ± 77.57[a]

[a] Averaged by three specimens.

Fig. 3. The TEM images of Ni05-1 and Ni05-2 sintered at 1250 °C for 3 min by SPS: (a), (c) and (d): Ni05-1; (b) Ni05-2.

alumina matrix leaving less at grain boundaries. Nickel particles at grain boundaries will block the growth of alumina grains and thus those in Ni05-2 are finer. In general, the refinement of grains is beneficial to toughness, but toughness is also greatly affected by other aspects of the microstructure. Microcracks and a large number of dislocations beside nickel particles are observed in images of Ni05-1 while only a few are seen in Ni05-2. Both of microcracks and dislocations improve the toughness of the composites [2]. Fig. 3(c) shows a local area in alumina grain of Ni05-1. As arrowed, a microcrack with a length of about 100 nm appears at the edge of a nickel particle inside the alumina grain. In Fig. 3(d), three dislocations longer than 200 nm appear just beside three nickel particles.

3.4. Toughening of the composites

Fig. 4 shows an instance of crack deflection (arrowed a) and the crack bridging of the nickel particles (arrowed b) in both composites; this is similar to Tuan's report [16]. The crack deflection model predicts a toughness increment of 12–15% [3] for uniformly distributed particles, which accounts for only a portion of the increase in toughness. The crack bridging of the nickel particles generally increases toughness greatly [8], but it affects the toughness of Ni05-1 and Ni05-2 similarly and cannot explain the toughness difference between Ni05-1 and Ni05-2. To solve this problem, the microstructures of Ni05-1 and Ni05-2 were studied by TEM. Microcracks and a high density of dislocations beside nickel particles are regularly observed in Ni05-1, but not in Ni05-2.

In this study, the microcracking is attributed to a mismatch of the thermal expansion coefficient between nickel and alumina. It decreases the elastic modulus of the crack-tip area, generates a nonlinear stress–strain relationship, redistributes the stress and toughens the ceramics. According to Davidge's theory [17], the critical grain size of the second phase, which could initiate
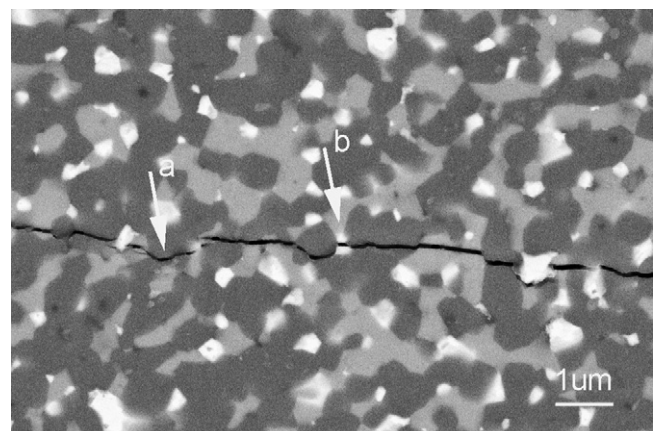

Fig. 4. Crack deflection of the Ni/Al$_2$O$_3$ composite.

microcracks, d_{cri}, is given by as follows:

$$d_{cri} = \frac{8\gamma_s}{P^2[(1 + \nu_c)/E_c + 2(1 - 2\nu_{me})/E_{me}]} \quad (1)$$

According to Sealing's [20] and Kolhe's [18] models, the thermal stress, P, due to the mismatch between matrix and the second phase, is given by

$$P = \frac{(\alpha_{me} - \alpha_c)\Delta T_s}{(1 + \nu_c)/2E_c + (1 - 2\nu_{me})/E_{me}} \quad (2)$$

where γ_s is the surface energy, here, 1.73 J/m^2 [22], ν the Poisson's ratio, α the thermal expansion coefficient, E the elastic modulus, the subscripts 'c' and 'me' represent the ceramic matrix and metal inclusion, here alumina and nickel respectively, and ΔT_s is the cooling range. The constants used in the formula are as follows: $\nu_c = 0.26$, $\nu_{me} = 0.31$, $\alpha_c = 8.4 \times 10^{-6}\,K^{-1}$, $\alpha_{me} = 13.2 \times 10^{-6}\,K^{-1}$, $E_c = 380\,GPa$, $E_{me} = 210\,GPa$, $\Delta T_s = 1230\,°C$.

Thus, P is given as 1.73 GPa by Eq. (2) and the critical grain size is 688 nm from Eq. (1). The nickel inclusions in this study are clearly below this critical value. The nickel particle size in Fig. 3(c) is about 300 nm and it initiates a microcrack. In Rolhe's report [18], a particle of 750 nm had initiated a crack whose size of the calculation is from 1.3 to 9.5 μm. It was pointed the residual tensile stress distribution and the particle geometries affected the results but did not attempt to take into account a more irregular shape. Real nickel inclusions in alumina ceramics will suffer form greater stress than the spherical particles in Sealing's model [20], especially acute edges such as that shown in Fig. 3(c). Davidge [17] also pointed out that stresses were magnified up to 1.4 times in the vicinity of the inclusions. Considering this factor, P in Eq. (1) could be much larger and the critical grain size could be close to the nickel particle size in Fig. 3(c). This may explain the difference between the calculation and the experimental result but no detailed residual tensile stress distribution modeling is performed in the present work.

Niihara [1] observed the sub-grain boundaries in SiC/Al$_2$O$_3$ nanocomposties and showed they were formed by the pinning and pile-up of dislocations by intragranular, hard SiC particles, which were generated in the Al$_2$O$_3$ matrix during cooling from the sintering temperature because of the highly localized thermal stresses within and/or around the SiC particles caused by the thermal expansion mismatch between Al$_2$O$_3$ and SiC. Similarly, many dislocations are seen in this study and a typical situation is shown in Fig. 3(d). The three dislocations are just beside the nickel particles and they are almost parallel. In contrast to those in Fig. 3(c), the nickel particles here are smaller (around 120 nm) and thus could not initiate a microcrack, but they can cause, or, at least affect, the formation of dislocations. Thus, dislocation pinning is considered an important factor in the toughening mechanism together with the microcrack toughening mechanism in Ni05-1.

4. Conclusions

Dense Ni/Al$_2$O$_3$ composites have been fabricated using the SPS method and the toughness of the composites is greatly improved compared to that of pure alumina. Microstructure observations reveal that the nickel dispersions in the composites are located both at grain boundaries and in grains. Microcracks caused by the mismatch between the alumina matrix and the metal inclusions, and also dislocations beside metal inclusions, are observed in Ni05-1, with a large percentage of nickel particles within alumina grains together with crack deflection and ductile particles bridging. The thermal stress and the critical grain size of the second phase, which could initiate microcracks, have been calculated. Microcracks and dislocation pinning toughen the composites, together with crack deflection and ductile particles bridging.

Acknowledgements

References

[1] K. Niihara, J. Ceram. Soc. Jpn. 99 (1991) 974–982.
[2] A. Nakahira, K. Niihara, J. Ceram. Soc. Jpn. 100 (1992) 448–453.
[3] K.T. Faber, A.G. Evans, Acta Metall. 31 (1983) 565–576.
[4] K.T. Faber, A.G. Evans, Acta Metall. 31 (1983) 577–584.
[5] M.F. Ashby, F.J. Blunt, M. Bannister, Acta Metall. 37 (1989) 1847–1857.
[6] B.D. Flinn, M. Rühle, A.G. Evans, Acta Metall. 37 (1989) 3001–3009.
[7] T. Ohji, Y. Jeong, Y. Choa, K. Niihara, J. Am. Ceram. Soc. 81 (1998) 1453–1460.
[8] F. Erdogan, P.F. Joseph, J. Am. Ceram. Soc. 72 (1989) 262–270.
[9] M. Taya, S. Hayashi, A.S. Kobayashi, H.S. Yoon, J. Am. Ceram. Soc. 73 (1990) 1382–1391.
[10] R. Kolhe, S. Tang, C.Y. Hui, A.T. Zehnder, Int. J. Solid Struct. 36 (1999) 5573–5595.
[11] J.S. Lu, L. Gao, J. Sun, L.H. Gui, J.K. Guo, Mater. Sci. Eng. A293 (2000) 223–228.
[12] T. Sekino, T. Nakajima, S. Ueda, K. Niihara, J. Am. Ceram. Soc. 80 (1997) 1139–1148.
[13] T. Sekino, K. Niihara, Nanostruct. Mater. 6 (1995) 663–666.
[14] A. Fnidiki, C. Dorien, F. Richomme, J. Teillet, D. Lemarchand, N.H. Duc, J.B. Youssef, H.L. Gall, J. Magn. Magn. Mater. 262 (2003) 368–373.
[15] O. Sbaizero, G. Pezzotti, Mater. Sci. Eng. A 343 (2003) 273–281.
[16] W.H. Tuan, R.J. Brook, J. Euro. Ceram. Soc. 6 (1990) 31–37.
[17] R.W. Davidge, T.J. Green, J. Mater. Sci. 3 (1968) 629–634.
[18] R. Kolhe, C.Y. Hui, E. Ustundag, S.L. Sass, Acta Mater. 44 (1996) 279–287.
[19] Y.M. Ito, M. Rosenblatt, L.Y. Cheng, F.F. Lange, A.G. Evans, Int. J. Fract. 17 (1981) 483–491.
[20] J. Seiling, J. Am. Ceram. Soc. 44 (1961) 419.
[21] G.J. Li, The synthesis and study of nano-NiO powders and Ni/Al$_2$O$_3$ cermet, Ph.D. Thesis, Shanghai Institute of Ceramics, Chinese Academy of Science, Shanghai, China, 2001.
[22] E. Saiz, R.M. Cannon, A.P. Tomsia, Acta Mater. 47 (1999) 4209–4220.